TÜBİTAK

Turkish Journal of Biology

http://journals.tubitak.gov.tr/biology/

Research Article

Turk J Biol
(2016) 40: 217-228
© TÜBİTAK
doi:10.3906/biy-1503-9

Production of recombinant human dipeptidyl peptidase IV from Sf9 cells in microbial fermenters

Özlem AYTEKİN[1,*], Saime İsmet DELİLOĞLU GÜRHAN[2], Kayoko OHURA[3], Teruko IMAI[3], Gaye ÖNGEN[2]

[1]Department of Food Engineering, Faculty of Engineering, Pamukkale University, Kınıklı, Denizli, Turkey
[2]Department of Bioengineering, Faculty of Engineering, Ege University, Bornova, İzmir, Turkey
[3]Graduate School of Pharmaceutical Sciences, Kumamoto University, Kumamoto, Japan

Received: 03.03.2015 • **Accepted/Published Online:** 26.06.2015 • **Final Version:** 05.01.2016

Abstract: The human dipeptidyl peptidase IV (hDPPIV/CD26) is expressed as an immune response in some cancer cells as well as intestine and incretin metabolism, and deficiency of the enzyme leads to metabolic disorders. In the present study, recombinant hDPPIV/CD26 genes were expressed in baculovirus–insect cell systems in a 5-L stirred-tank fermenter. Because of the shear sensitivity of the insect cell line, production from insect cells should be performed in new-generation type bioreactors, which are commonly more expensive than microbial fermenters. To optimize the process, hydrodynamic parameters and oxygen consumption of Sf9 cells at 1.5 L and 3 L were monitored, and a certain amount of serum was added to the production medium to decrease shear and stabilize the growth of insect cells that normally do not need serum addition. In this study, dimensionless numbers and some hydrodynamic parameters were calculated in 1.5 L, and predictions were made for 3 L fermenter volumes. Agitation rates of 60 rpm were determined to protect insect cells against damaging shear stress. Regarding the agitation rate, oxygen mass transfer coefficient (k_La) was 0.0129 min^{-1} for 1.5 L and was kept constant for 3 L (0.0133 min^{-1}). The maximum enzyme activity from microbial fermenters was 2.37-fold higher than activity from T-flask in our previous work. The infection efficiency of transfected cells was 78%–81% in the 1.5-L and 3-L fermenters.

Key words: Human dipeptidyl peptidase IV, *Spodoptera frugiperda* (Sf9), microbial fermenter, recombinant protein production

1. Introduction

Human dipeptidyl peptidase IV (hDPPIV/CD26, EC 3.4.14.5) is a member of the type II transmembrane serine proteases that cleave the N-terminal dipeptides X-Pro or X-Ala from target polypeptidase, such as peptide hormones and chemokines. DPPIV is expressed in microbial and insect cells and nearly all mammalian tissues (Cunningham and O'Connor, 1997), and it plays important roles in the gastrointestinal, neurological, endocrinological, and immunological systems (Demuth and Heins, 1995; Bergmann and Bohuon, 2002; Thoma et al., 2003; Pérez-Guzmán et al., 2004). This enzyme regulates blood sugar levels and overexpresses in cancer cells and tumor progression in several human malignancies; in addition, lack of the enzyme reportedly causes autoimmune diseases (Reichelt et al., 1981; Shattock et al., 1990; Iwaki-Egawa et al., 1998; Langford, 2000; Bergmann and Bohuon, 2002; Lambeir et al., 2002; Reichelt and Knisberg, 2003; Aertgeerts et al., 2004; Urade et al., 2006).

Currently, DPPIV is widely used as an important compound in commercial digestive enzymes to support patients who lack the hydrolysis enzyme (Üstün and Öngen, 2012). Studies have shown that bacterial production of DPPIV is the most economical method due to the short incubation periods required, such as 4–6 h in submerged culture (Zevaco et al., 1990; Lloyd and Pritchard, 1991; Tachi et al., 1992; Wilkinson and Houston, 2001; Ota et al., 2005; Üstün and Öngen, 2012). However, certain portions of the enzyme expressed in prokaryotes may be of limited use in human metabolism due to the potential for improper posttranslational modifications. Therefore, Aspergillus strains are commonly preferred for the commercial production of extracellular DPPIV in the dietary supplement market (Tachi et al., 1992; Doumas et al., 1998; Öngen et al., 2012). In addition to fungi, mammalian cells and insect cells also offer feasible eukaryotic hosts for dietary supplement production.

Insect cell and baculovirus expressions are known to be industrially useful systems for recombinant protein production. Certain technological advances are much easier to culture in animal cells due to their higher tolerance for osmolality, by-product concentrations, proper posttranslational modifications, and higher expression levels (Ikonomou et al., 2003). Additionally,

* Correspondence: drozlemaytekin@gmail.com

insect cells can easily adapt to industrial media from adherent to suspension cultures in shake flasks and bioreactors (Jianyong et al., 1990).

Most related studies have focused on expression, characterization, and purification techniques to determine the biological structure of hDPPIV/CD26 using various small-scale resources, such as T-flask or shake-flask cultures (Yamaji et al., 1999; Dobers et al., 2002; Carmo et al., 2012). Rice et al. (1993) reported that a stirred-vessel fermenter could be an alternative recombinant protein production system for Sf9 cell growth and protein expression levels. In this study, the production of an Sf9 insect cell line from a T-flask to a 3-L stirred fermenter and the expression of recombinant hDPPIV/CD26 were examined in serum-added medium to protect the cell line against the detrimental effects of shear stress.

Determination of the optimal viral titer is critical for achieving a high expression level and productivity in a recombinant protein. Therefore, in traditional batch fermentation processes high multiplicity of infection (MOI) values for the two scaling-up processes should be considered: one for the cell and one for the virus. However, low-MOI strategies lead to the preservation of the genetic integrity of a virus due to the low passage effects. In the present study, our low-MOI strategy was examined for high expression and productivity of hDPPIV/CD26 from Sf9 cells in 1.5-L and 3-L fermenters.

Oxygen consumption, cell viability, and enzyme expression were monitored in a stirred-tank fermenter, which is traditionally preferred in industrial production due to the low economic and design demands involved. Agitation rates, aeration rates, and shear stress were determined for the Sf9 cells.

2. Materials and methods

2.1. Materials

The Spodoptera frugiperda cell line (Sf9), pFastBac1 transfer vector, competent DH10Bac Escherichia coli cells, Sf-900 II SFM, Cellfectin II, and antibiotics were purchased from Invitrogen, Gibco BRL. Bluo-Gal, IPTG, protease inhibitor mix, and EX-CELL 420 medium were obtained from Sigma.

2.2. Plasmid construction, transfection of bacmid DNA into Sf9 cells, and amplification of recombinant baculovirus

The full-length cDNA of hDPPIV/CD26 was obtained from pEBFP-N1-DPP IV (University of Magdeburg, Germany), and all routine restriction enzyme digestion and ligation was performed into the cloning site of pFastBac1 (Gibco BRL) vector (Üstün-Aytekin et al., 2014). The recombinant plasmid was transformed from pFastBac1 to E. coli DH10Bac, and bacmid DNA was extracted by HiSpeed Plasmid Maxi kit (Qiagen, Germany). Monolayers of Sf9 cells (9×10^5 cells per well in a 6-well plate) were transfected with purified bacmid-DNA using the Cellfectin II reagent (Gibco BRL). The recombinant virus was amplified twice to obtain higher titered virus stocks and then harvested. Virus titers were determined by plaque assay (Celis et al., 2005).

2.2.1. hDPPIV/CD26 protein expression and preparation of baculovirus-infected cell stocks

Sf9 cells in 6-well plates [Sf-900 II SFM, 10% v/v heat-inactivated fetal bovine serum (FBS, Biochrome, Germany) and 50 μg mL^{-1} w/v, gentamicin] were infected with recombinant viruses at MOI values of 0.1 using the harvest time (72 h) reported in our previous study (Üstün-Aytekin et al., 2014). Infected cells (1×10^7 cells) were cryopreserved as baculovirus-infected cell stocks and stored at –86 °C (Wasilko and Lee, 2006). The infected cells (1×10^6 viable cells) were quickly thawed and inoculated into the fermenter (Wasilko et al., 2009).

2.3. Disruption of infected Sf9 cells

The infected cells were washed three times with phosphate-buffered saline (PBS) and then resuspended on ice in 300 μL of lysis buffer [20 mM Tris-HCl (pH 8.0), 300 mM NaCl, 10% (w/v) glycerol, IPEGAL CA-630] for 9×10^5 cells mL^{-1}. Samples were centrifuged for 10 min at 12,000 × *g* at 4 °C after sonication (three 20-s pulses with the Bandelin model, 45% power). The supernatants were examined for hDPPIV/CD26 activities and protein amounts or stored at –20 °C until further use.

2.4. Determination of protein concentration, enzymatic activity, and electrophoretic mobility of proteins

The protein concentrations were assayed using the BCA Protein Assay Reagent kit (Pierce). Enzymatic activity was determined with Gly-Pro-p-nitroanilide as the substrate. The amount of the enzyme producing 1 μmol p-nitroaniline per minute was defined as the unit of enzyme. The production samples were analyzed by SDS-PAGE according to the method of Laemmli (1970). Molecular weight marker proteins (molecular weight standard 10–250 kDa; Fermentas, Canada) were used as references.

2.5. Monitoring hDPPIV/CD26 expression with immunofluorescence method

The fluorescence method was used to detect the location and relative abundance of the hDPPIV/CD26 enzyme. CD26 rabbit polyclonal antibody (CD 26-H270: sc-9153; Santa Cruz, USA) was used as the primary antibody, and goat anti-rabbit (594; Invitrogen, UK) was the secondary antibody. The cells were fixed to coverslips and washed three times in 500 μL of PBS for 5 min, 1 mL of blocking solution (PBS/triton X-100) was added, and the cells were incubated for 1 h at room temperature. The cells were resuspended in 50 μL of primer antibody (PBS/triton

X-100, 1:100) overnight at 4 °C. After washing three times in PBS, the cells were resuspended in secondary antibody (PBS/triton X-100, 1:750) for 2 h at room temperature. The cells were exposed to an appropriate amount of 4',6-diamidino-2-phenylindole for 20 min and washed three times in PBS. The cover slips were sealed with paraffin and the labeled cell preparations were examined with a Leica DM IL LED (Germany) confocal microscope.

2.6. Adaptation of Sf9 cells to EX-CELL 420 medium

Because uninfected Sf9 cells are not able to adapt directly from adherent culture media into new media designed for use in large scale production, the growth medium was gradually switched from Sf-900 II SFM [10% v/v, heat-inactivated FBS, and gentamicin (w/v, 50 μg mL^{-1})] to EX-CELL 420 medium [10% v/v, heat-inactivated FBS, and gentamicin (w/v, 50 μg mL^{-1})] to prepare the adherent Sf9 cell culture in T-flasks. Sf-900 II SFM-adapted cell lines were maintained in approximately 75% Sf-900 II SFM and 25% EX-CELL 420 for two passages. Next, the medium was replaced with approximately 50% Sf-900 II SFM and 50% EX-CELL 420 for two passages. In the last step, the medium was replaced with approximately 25% Sf-900 II SFM and approximately 75% EX-CELL 420. Finally, the 100% used in industrial production was attained. The morphology of the cell lines was monitored under an inverse phase microscope after each medium replacement (Figure 1). Although the preferred media have been formulated as serum free, FBS (10% v/v, heat-inactivated) was added to protect the cells against the hydrodynamically lethal effect from Rushton turbines.

2.7. Inoculum preparation

After adapting the uninfected Sf9 cells to EX-CELL 420 medium, the cells were routinely maintained in 125-mL shake flasks at a working volume of 20 mL of EX-CELL 420 [10% v/v heat-inactivated FBS and gentamicin (w/v, 50 μg mL^{-1})] at 27 °C and then agitated at 90 rpm. The cell densities were determined using a hemocytometer, and the viability was determined by the trypan blue dye exclusion method.

These pre-adapted cells were subcultured to 4–5 × 10^5 viable cells mL^{-1} after reaching 1 × 10^6 cells mL^{-1} in 20 mL of EX-CELL 420 medium.

2.8. Fermenter conditions and Sf9 cell line propagation

A stirred-tank bench top microbial fermenter (5 L; Sartorius Stedim, Biostat B, Germany) was used in batch mode to express hDPPIV/CD26 in the Sf9 cells. The fermenter, which was constructed of glass and equipped with Rushton type impellers, was run first at a working volume of 1.5 L and then at 3 L. The fermenter containing distilled water was autoclaved at 15 psig and 121 °C for 45 min.

The dissolved oxygen (DO) concentration was monitored during production to determine oxygen consumption. The medium used in the fermenter cultures was EX-CELL 420, supplemented with FBS and gentamicin. The fermenter was seeded with exponentially growing cells at an initial concentration of 4–5 × 10^5 viable cells mL^{-1} from the shake flask cultures under sterile conditions. The cultures were infected with baculovirus-infected cell stocks (MOI of 0.1) when the cells reached a level of 1 × 10^6 viable cells mL^{-1} in the fermenter.

During this process, as well as before and after infection, the fermenter was monitored for pH, cell viability, hDPPIV/CD26 activity, and the amount of protein, in addition to oxygen consumption. Therefore, culture samples were taken at regular intervals from the fermenter and centrifuged. The cell pellets were resuspended in a lysis buffer, disrupted, and centrifuged. After centrifugation, the clear supernatant samples were stored at –20 °C for subsequent analysis.

2.9. Strategies of production in microbial fermenter

Aeration rate (Q), specific death rate) (k_d), agitation rate (N), and shear stress (t) were considered when scaling up from the flask to the 1.5-L-working-volume fermenter. Calculation steps were estimated for every rotational speed of the impeller from 40 to 100 rpm, and one was selected based on its possible shear stress for 1.5 L and 3 L scale production (Aiba et al., 1973; Doran, 1995; Wu and Goosen, 1995; Tramper et al., 1996).

The scale-up of production was designed with the oxygen mass transfer coefficient (k_La) principle. The production of Sf9 cells was monitored for oxygen transfer rate (OTR), oxygen uptake rate (OUR), specific oxygen consumption rate (q_{O2}), and k_La by ensuring optimal rotational speeds of the impeller and optimal aeration rates at a working volume of 1.5 L for 15 days. The specific oxygen consumption rate (q_{O2}) was determined by following the amount of dissolved oxygen in the medium when the gas supply to the fermenter was turned off; thus, q_{O2} can be calculated as follows (Gomez et al., 2006):

$$\frac{dC}{dt} = q_{02} C_x = OUR\,. \qquad (1)$$

In Eq. (1), is the biomass concentration (cell mL^{-1}), and dC/dt is the accumulation of oxygen in the liquid phase. The dissolved oxygen concentration gradually increased up to a constant value after aeration was restarted, and k_La was determined with the estimated OUR value. Oxygen transfer is usually limited by the liquid film surrounding the gas bubbles. The rate of transport is given by the following equation:

$$\frac{dC}{dt} = OTR - OUR = k_L a(C_L^* - C_L)\,, \qquad (2)$$

where k_L is the oxygen transport coefficient (cm h^{-1}), a is the gas-liquid interfacial area ($cm^2\,cm^{-3}$), the oxygen mass transfer coefficient (h^{-1}), the saturated DO concentration

(mg mL^{-1}) (approx. 8 mg mL^{-1} at 25 °C and 1 atm), and is the actual DO concentration in the liquid (mg mL^{-1}) (Bailey and Ollis, 1986). The value was kept constant during production from the 1.5 L fermenter to the 3 L fermenter [Eq. (3)] by considering the OTR and OUR in the 1.5 L fermenter:

$$k_L a = 2x10^{-3}(\frac{P}{V})^{0.7} u_G^{0.2}. \quad (3)$$

2.10. Separation steps for recombinant hDPPIV/CD26

Samples were taken daily from the fermenter and centrifuged at 100 × *g* for 5 min at 4 °C using the Sigma 3K30 (Newtown, UK). Then samples were washed three times with PBS and centrifuged under the same conditions. After removing the supernatant, the cells were disrupted by sonication in lysis buffer and centrifuged at 12,000 × g for 10 min. The crude cell extract was applied to the ion exchange column (Hiprep 16/10 QFF, GE Healthcare) and equilibrated with 100 mM Tris–HCl (pH 9.0) buffer. Proteins were eluted at 1 mL min^{-1}, applying an initial isocratic step to the equilibration buffer, followed by a linear gradient from 0 to 2 M NaCl. The eluate was collected in 4-mL fractions. The active samples were applied to a Sephacryl 300 HR column (GE Healthcare), which is a molecular size exclusion column, and equilibrated with 100 mM Tris–HCl (pH 9.0). The proteins were eluted at 0.3 mL min^{-1}, and 5-mL fractions were collected and stored at –20 °C until further use.

3. Results

3.1. Production in microbial fermenter: adaptation of Sf9 cells to the industrial media and propagation of the cells in shake flasks

The nonadapted cell lines evolved into a polymorphic shape; the cells lost their adherent ability after direct replacement with EX-CELL 420 (Figure 1). Infection of these nonadapted cells (Figure 1) may affect gene expression and cell growth kinetics. Therefore, the adaptation of the cells in the new medium and cell maintenance must be accomplished before large scale production. As shown in Figure 1b, the cells were attached firmly to the T-flask surface; the size of the cells was small and regular. Progressive adaptation of Sf9 cells was successfully achieved.

3.2. Production strategies in the microbial fermenter: calculation of bubble size, specific death rate, and aeration rate

In the present study, the injected bubble size (from the ring sparger to the fermenter was calculated as 3.5 mm according to Doran (1995). and were calculated and examined considering the recommended aeration range 0.005–0.007 vvm in sparged bioreactors, according to Jöbses et al. (1991) and Doran (1995). The values were calculated as = 2.20 × 10^{-7} s^{-1} (0.005 vvm) and = 8.81 × 10^{-7} s^{-1} (0.03 vvm) for the 1.5-L and 3-L fermenters, respectively, in the present study.

Sparging-associated damages can be enhanced by impeller agitation. Therefore, other hydrodynamic forces, including agitation rate and shear stress values, were also calculated.

3.3. Production strategies in the fermenters: dimensionless numbers, shear stress, and agitation rate

Dimensionless numbers and some hydrodynamic parameters related to the viscosity and density in the 1.5-L fermenter are given in Table 1. The impeller Reynolds number indicated that the flow regime was turbulent in the stirred-tank fermenter. Power number (P_{no}) was 5 according to the graph of Aiba et al. (1973), which represents the power number versus the Reynolds number for Rushton turbine geometry. There has been a significant connection between sparged gas and power consumption in the aerated fermenter. The gassed power consumption

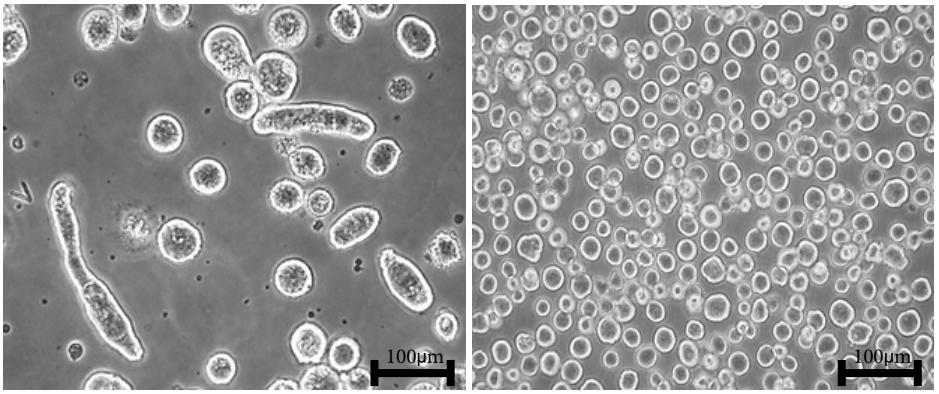

(a) (b)

Figure 1. a) Nonadapted Sf9 cells from Sf-900 II SFM to EX-CELL 420, b) Sf9 cells pre-adapted to EX-CELL 420 (20×; Olympus, Japan).

Table 1. Dimensionless numbers and some hydrodynamic parameters in the 1.5-L fermenter.

Total volume (L)	5
Operating volume (L)	1.5
μ (kg m^{-1} s^{-1})	1.122×10^{-3}
ϑ (m^2 s^{-1})	1.1×10^{-6}
Re_i	3272
P_{no}	5
N_a	5×10^{-4}
P_g/P	0.95

decreased (P_g), as the sparged gas bubbles reduced the liquid density in the aerated fermenters (Hensirisak et al., 2002). P_g is a function used to calculate the empirical mass average of turbulent energy dissipation (ε) based on the energy dissipation equality; ε was used to calculate maximum shear stress (τ_{max}) (Table 2).

3.4. Monitoring Sf9 cell propagation and hDPPIV expression in fermenters

The adapted uninfected Sf9 cells with EX-CELL 420 were inoculated into the 1.5-L working volume and treated with baculovirus-infected cell stocks (MOI of 0.1) when the concentration of cultured Sf9 cells reached 8×10^5 cell mL^{-1}. The hDPPIV activity and percent cell viabilities are shown in Figure 2. The doubling time of the uninfected cells was 26 h, and the specific growth rate was 0.026 h^{-1} in the fermenter. After infection at 48 h, the Sf9 cells grew gradually up to 96 h, followed by a significant decrease until the number of infected cells was attained in a stable stationary phase. The expression of hDPPIV/CD26 increased 39-fold over the same period. The amount of protein in the same samples was 7 mg mL^{-1} and 9 mg mL^{-1} at 24 h and 144 h, respectively. Viable cell counts and the amount of expressed hDPPIV/CD26 had opposite correlations until 168 h postinfection, at which point both had reached a steady state. Therefore, the expression of recombinant hDPPIV/CD26 (575.49 mU mL^{-1} ± 28.7) from infected cells was thought to remain stable, despite the passage of time and formation of by-products.

The propagation of Sf9 cells was achieved by maintaining a constant when increasing the volume from 1.5 L to 3 L. The doubling time of uninfected cells was 51 h, and the specific growth rate was 0.01 h^{-1}.

As shown in Figure 2, the increasing expression of hDPPIV/CD26 activity and the decreasing cell viability of infected Sf9 cells in the 3-L reaction had similar propensities in the 1.5-L reaction. Cell count became 5×10^4 cells mL^{-1} after 216 h and 312 h in 1.5-L and 3-L fermentation, respectively. The time difference between these productions were due to the restrictions resulting from agitation and aeration rates. As mentioned above, the agitation rate can be adjusted to a maximum 60 rpm, and aeration was adjusted for k_La, which should be same in both productions. However, due to V_k and the shear effect there was also a limitation for aeration. The expression of hDPPIV/CD26 (639.25 mU mL^{-1} ± 30.95) increased slightly at 216 h postinfection and then remained constant up to the end of production in the 3-L fermenter. hDPPIV/CD26 was 29-fold higher at 360 h than at 0 h, while the protein amounts of the samples were 6.42 mg mL^{-1} and 6.24 mg mL^{-1} at 0 h and 216 h, respectively.

The expression of hDPPIV/CD26 was supported by SDS-PAGE in Figure 3. The density of the expressed hDPPIV/CD26 bands on SDS-PAGE supported the amount of hDPPIV activity from infected Sf9 cells in both the 1.5-L and 3-L preparations. The molecular weight of hDPPIV was measured taking into consideration the electrophoretic mobility of proteins and markers on the gel and was approximately 70 kDa (69.19 kDa).

Table 2. Possible shear stresses at increasing agitation rates in the EX-CELL 420 medium.

	Agitation rates						
	40 rpm	50 rpm	60 rpm	70 rpm	80 rpm	90 rpm	100 rpm
P_g ($\frac{kgm^2}{s^3}$)	0.0010	0.0021	0.0037	0.0059	0.0095	0.0128	0.0173
ε ($\frac{m^2}{s^3}$)	0.0047	0.0095	0.0168	0.0267	0.0432	0.0583	0.0790
τ_{max} ($\frac{N}{m^2}$)	0.39	0.55	0.73	0.93	1.18	1.37	1.60

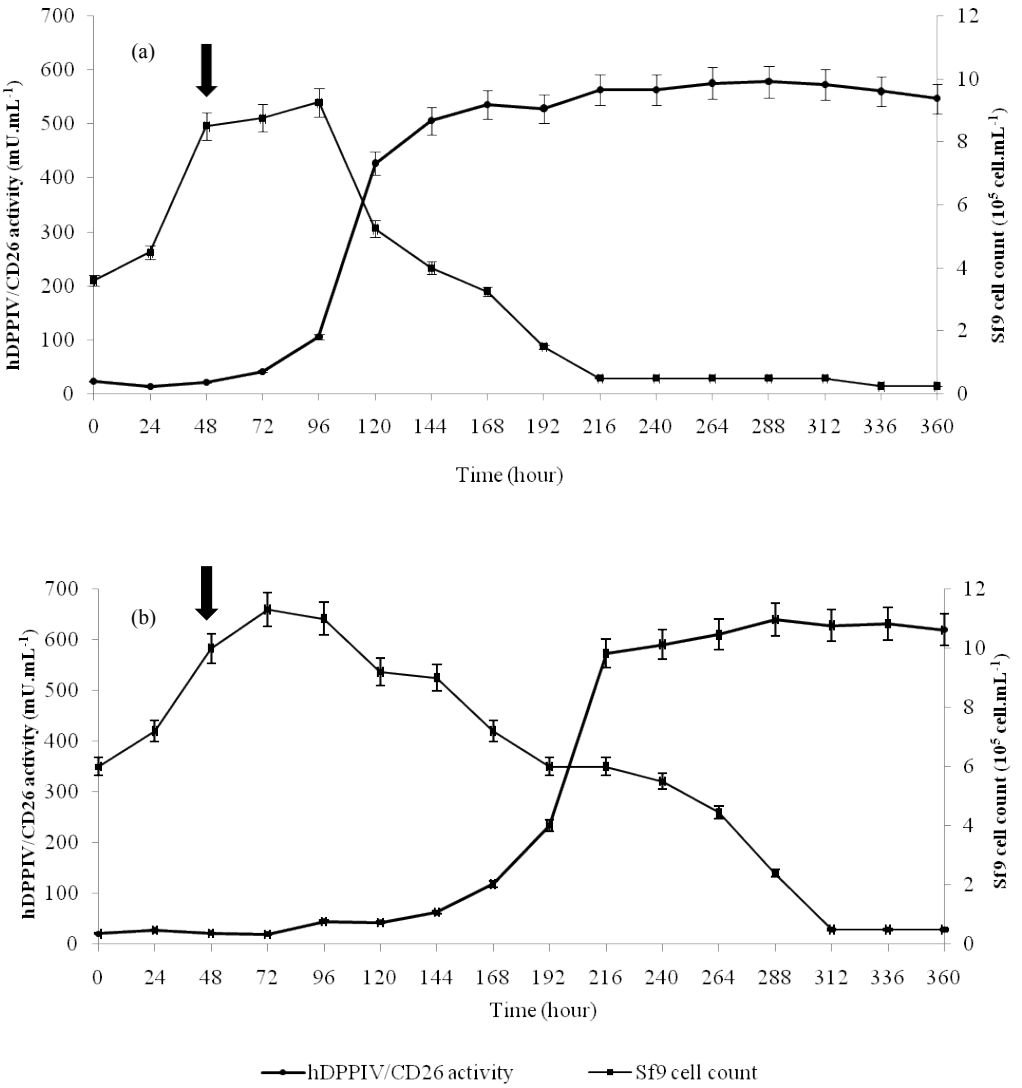

Figure 2. Expressed hDPPIV/CD26 activity (●), infection time (black arrow), and viable count of Sf9 cell (■) variation with time over a 15-day batch culture in a 1.5-L (a) and 3-L (b) stirred-tank fermenter.

3.5. Oxygen consumption in the 1.5-L and 3-L productions

Varying states of oxygen consumption among the uninfected and infected Sf9 cells were observed (Table 3). The oxygen consumption values (OUR and q_{O2}) increased approximately 2.4-fold at 72 h postinfection in the 1.5-L fermenter. The data from the 3-L fermenter also supported this result.

The scale-up equations were performed to keep k_La values constant at the 1.5-L and the 3-L scales. As a result of these equations k_La values were 0.0129 min^{-1} and 0.0133 min^{-1}, respectively.

3.6. Infection efficiency and productivity of hDPPIV/CD26 in the 1.5-L and 3-L reactions

The immunofluorescence results revealed that infection efficiency, that is, the percentage of transfected Sf9 cells in the population, was 78%–81% in the 1.5-L and 3-L fermenters. Moreover, the ratio of hDPPIV/CD26 expressing infected cells (Figure 4) to total infected cells was 96% at the 1.5-L scale and 90% at the 3-L scale.

The productivity values of the 1.5-L reaction at 120 h and the 3-L reaction at 216 h were 3.56 mU mL^{-1} h^{-1} (during the first 48 h of cell growth) and 2.98 mU mL^{-1} h^{-1} (during the first 48 h of cell growth), respectively. The

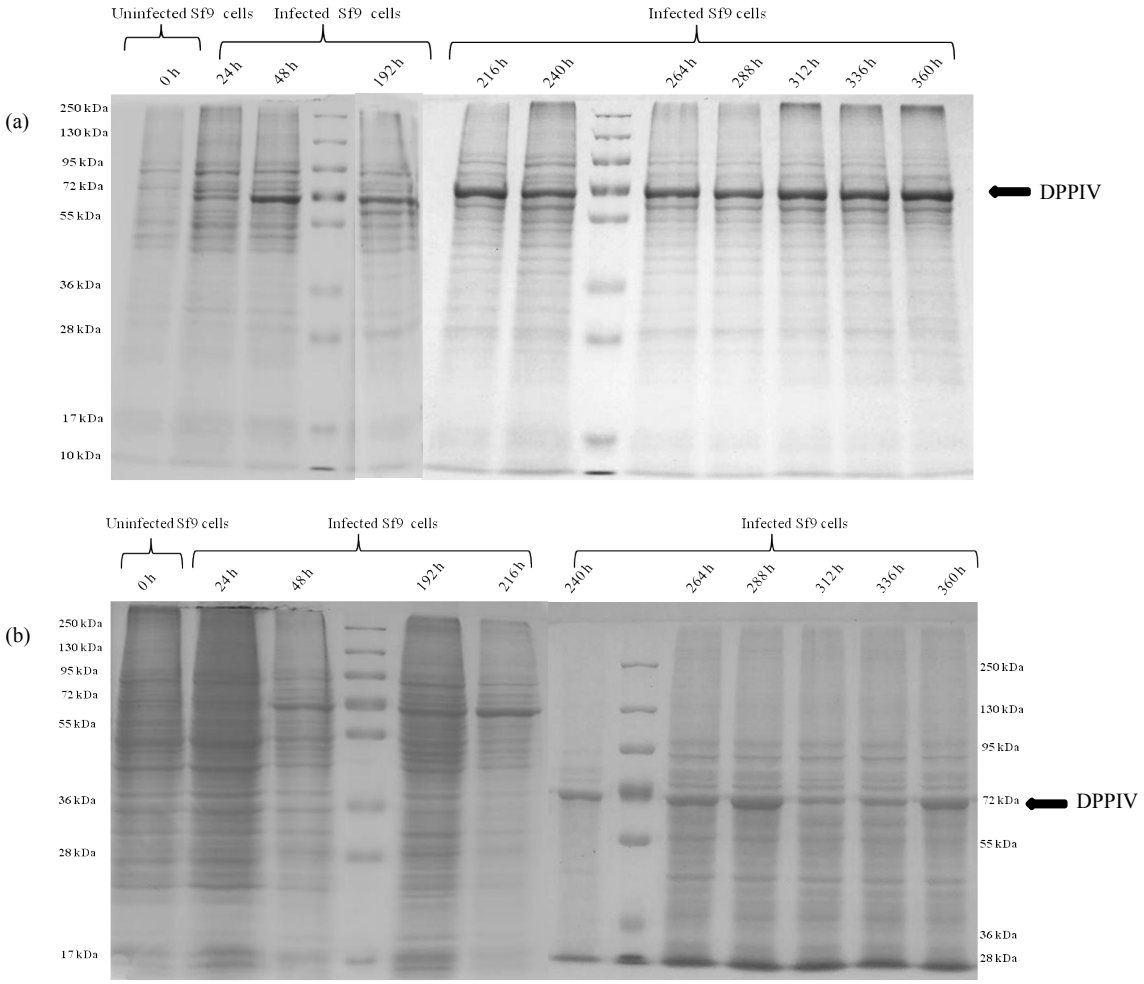

Figure 3. Analysis of the hDPPIV/CD26 expression of Sf9 cells in fermenters. (a) hDPPIV/CD26 expression from Sf9 cells in the 1.5-L fermenter, (b) hDPPIV/CD26 expression from Sf9 cells in the 3-L fermenter. Lanes 4 and 8: prestained molecular weight markers (Fujifilm, Finepix F 200 EXR, Japan).

Table 3. OTR, OUR, q_{O2}, and hDPPIV activity for infected and uninfected Sf9 cells at two different working volumes (1.5 L and 3 L) in the 5-L fermenter.

	0 h (uninfected Sf9 cells)	72 h postinfection (infected Sf9 cells)	240 h postinfection (infected Sf9 cells)
qO_2 ($molO_2\ cell^{-1}\ s^{-1}$)			
1.5 L 3 L	9.37×10^{-17} 11.35×10^{-17}	22.6×10^{-17} 17.5×10^{-17}	22.1×10^{-17} 26.5×10^{-17}
OUR ($mgO_2\ L^{-1}\ min^{-1}$)			
1.5 L 3 L	0.065 0.2181	0.2284 0.3696	0.0213 0.0255
Cell count (cell mL^{-1})			
1.5 L 3 L	3.6×10^5 10×10^5	5.25×10^5 11×10^5	0.5×10^5 0.5×10^5
hDPPIV (mU mL^{-1})			
1.5 L 3 L	23.6 17	427.06 63.08	563.01 631.15

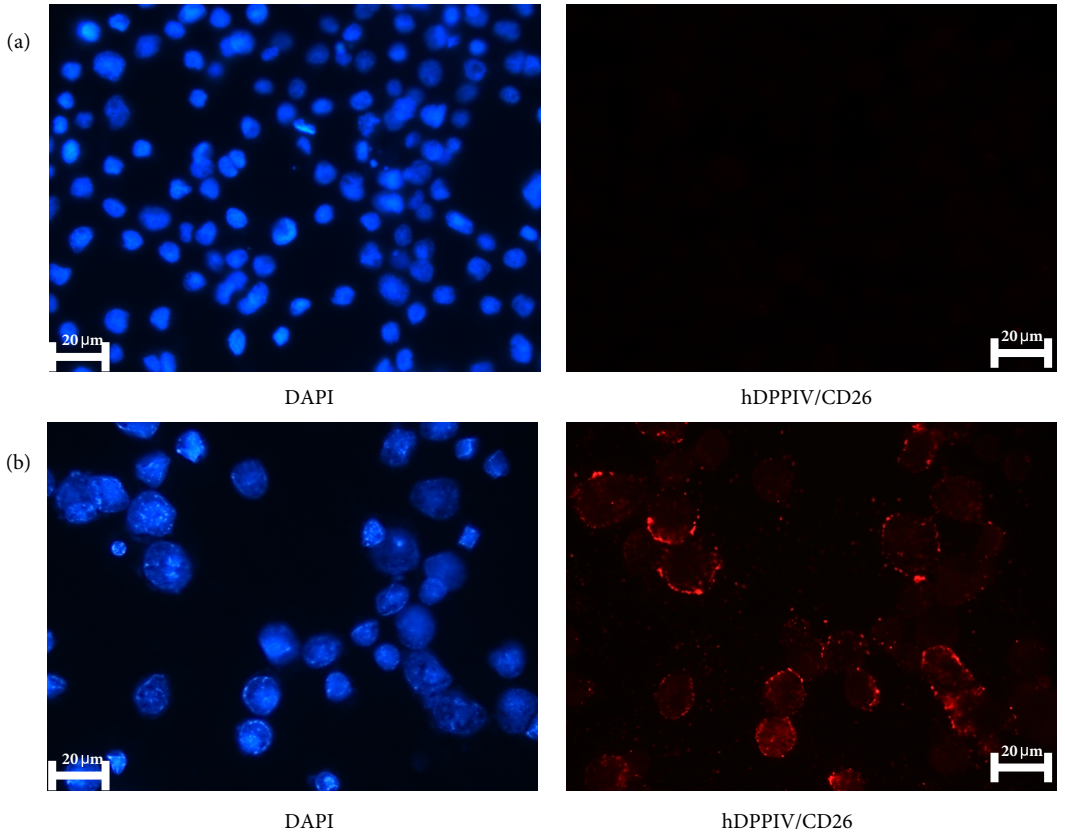

Figure 4. Immunofluorescence images of recombinant hDPPIV/CD26 proteins expressed from Sf9 cells. (a) Uninfected cells, (b) baculovirus infected (MOI = 0.1) Sf9 cells at the end of fermenter production (1.5 L), (66X, Leica DM IL LED, Germany).

number of cells infected with recombinant baculovirus at a MOI of 0.1 was 0.5–6 × 10^5 cell mL^{-1} on these scales.

3.7. Separation processes of recombinant hDPPIV/CD26

Purification of the expressed hDPPIV/CD26 protein was carried out in two chromatographic columns. Infected Sf9 cells were disrupted and centrifuged, and then the cleared lysates were loaded through to the first column (HiPrep 16/10 QFF), which was an anion exchange column that yielded major peaks on the chromatogram (data not shown). Recombinant hDPPIV/CD26 was purified as a sharp and clear peak from the column. All fractions were tested for hDPPIV/CD26 activity, and the fractions with high hDPPIV/CD26 activity (22nd fraction) were applied to a second column of HiPrep Sephacryl 300 HR (data not shown).

The maximum recombinant hDPPIV/CD26 activity was eluted in the 8th fraction from the molecular size exclusion column. Further, the eluate was purified from the column as a single peak.

4. Discussion

4.1. Production strategies in the microbial fermenter: calculation of bubble size, specific death rate, and aeration rate

A commonly held belief is that the hydrodynamic forces (such as shear stress) associated with agitation and aeration may be detrimental to animal cells. One of the most significant challenges in suspension cultures of mammalian and insect cell lines is shear sensitivity, as these cell lines are very fragile due to their relatively large size and lack of a cell wall (Garcia-Briones and Chalmers, 1992; Tramper et al., 1996). In particular, when the process is conducted in microbial fermenters, hydraulic pressure caused by liquid height becomes significant for sensitive cells. Therefore, in addition to the proper aeration rate and specific death rates in sparged fermenters, determination of bubble size is important for growing the cells. Bubbles are defined in a fermenter as large or small. Large bubbles rise faster and carry fewer attached cells to the surface

compared with small bubbles. According to a study on hybridoma cells by Handa et al. (1987), small bubbles were more detrimental to cells than the larger ones due to their high energy dissipation capacity. In the present study, the injected bubble size from the ring sparger to the fermenter was 3.5 mm, and this bubble size was considered large by Bavarian et al. (1991).

The cell damage of bubble size may differ depending on the cell types, and cell damage is affected by hypothetical killing volumes [for insect cells in 10% fetal bovine serum (FBS) supplemented media, Vk =m^3],, and aeration rate (Tramper et al., 1996). Wu and Goosen (1995) reported that there was an adverse correlation between $k_La - k_d$, $- k_d$ height of fluid in fermenters (D_b), and $- V_k$. Eibl et al. (2009) reported that the values of should be low in the bioreactor for the protection of cells against aeration rate damage, and Chisti (2000) found that the ideal was 5×10^{-5} s^{-1} for insect cells with large bubbles in serum-free medium. The values from the present study are lower than those in related studies. Therefore, we clearly see that medium with serum showed a significant effect on cell viability in the fermenter compared to the literature. Beas-Catena et al. (2013) found that cell concentration and growth rates of serum-containing medium decreased by about 50%, and the viabilities diminished to 83%–84% in serum-free medium. Serum-free medium may be economically feasible, but every cell line may not grow in it.

4.2. Dimensionless numbers, shear stress, and agitation rate

The values of shear stress increased with the agitation rate (Table 2). Tramper et al. (1996) indicated that a shear stress of approximately 1 N m^{-2} was the critical value for insect cell damage, and Agathos et al. (1996) reported that the viability of insect cell cultures decreased with shear stresses of 1.5 N m^{-2} and 3 N m^{-2} on two different runs. Agitation rates (higher than 70 rpm) may have detrimental effects in insect cells. In the case of 50 rpm, agitation is not sufficient to maintain a uniform distribution of cells in the fermenter; instead, a large clump grew at the bottom of the fermenter. Therefore, the optimal agitation rate was determined at 60 rpm using the 0.005 vvm aeration rate in the 1.5-L stirred-tank fermenter.

4.3. Oxygen consumption in 1.5-L and 3-L productions

Oxygen consumption may differ, depending on the cell line, and this is a vital parameter for infection processes. However, the determined specific oxygen consumption rates were similar between insect and mammalian cells (Schmid, 1996). As shown in Table 3, the oxygen consumption obtained in this work was between 9.37×10^{-17} mol cell^{-1} s^{-1} and 11.35×10^{-17} mol cell^{-1} s^{-1} in the 1.5-L and 3-L fermenters, respectively. Oxygen consumption in insect cells has been reported at $3.5–9.9 \times 10^{-17}$ mol cell^{-1} s^{-1} under different conditions (Kioukia et al., 1995). This difference arises due to the absence of serum in the medium. Reuveny et al. (1992) reported that specific OURs (q_{O2}) of the Sf9 cells, varying between the serum-containing medium (glucose and 10% fetal calf serum) and the serum-free medium (ICSF-WB, BioWhittaker), were 6.1×10^{-17} mol cell^{-1} s^{-1} and 12×10^{-17} mol cell^{-1} s^{-1}, respectively. This oxygen uptake rate should be sustained by elevated aeration rates, which may also affect the growth of cell line due to shear stress.

Most research groups have reported that the oxygen demands of insect cells increase after infection, and this property may be responsible for differences arising in using the wild-type baculovirus expression vectors, MOI values, and physiological condition of the cells between the time of infection and the period of the infection (Schmid, 1996; Palomares and

Ramirez, 1996; Radner et al., 2012). The oxygen consumption values (OUR and q_{O2}) in the present study supported these related studies. Increased q_{O2} indicated expression of recombinant hDPPIV/CD26 proteins 72 h and 240 h postinfection (Table 3). The addition of serum to insect cell line medium helps to decrease the level of OURs and shear stress.

In addition to oxygen consumption values, plays an important role in maintaining the economy of the processes, scaling up, and process design for aerated production (Alam and Razalı, 2005). Measured kLa values indicate that the theoretical calculations are supported by measured data.

4.4. Monitoring of hDPPIV expression in fermenters

The maximum enzyme activity from the microbial fermenters in the present study was 2.37-fold higher than in a T-flask (269 mU mL^{-1} ± 13.45) in a previous work (Üstün-Aytekin et al., 2014). Despite the increasing expression of recombinant hDPPIV/CD26 activity, the similar protein amounts indicated that recombinant hDPPIV/CD26 expression was accomplished successfully. The molecular weight of the enzyme was consistent with the predicted molecular mass from the amino acid sequence of hDPPIV/CD26 (2300 bp) (Tanaka et al., 1992; Thoma et al., 2003; Üstün-Aytekin et al., 2014).

4.5. Infection efficiency and productivity of hDPPIV/CD26 in the fermenters

Two phenomena are critical for the successful and fast expression of an animal cell line in a large scale: infection efficiency and productivity. Higher infection efficiency values (90% and 96% for 1.5 L and 3 L, respectively) of recombinant hDPPIV/CD26 were achieved in the present study than in related studies in which the infection efficiency was approximately 20%–30% of Sf9 and Sf21 cells at 72 h (Radner et al., 2012), while Pham et al. (2003) noted an infection efficiency at 40%–60%. The high infection efficiency and short incubation period contributed to the

Table 4. Separation steps of hDPPIV from baculovirus-infected Sf9 insect cells (100 mL of monolayer culture, 8×10^5 cell mL^{-1}).

Steps	Total protein (mg)	Total activity (mU)	Specific activity (mU mg^{-1})	Yield (%)	Purification fold
Cell lysate	70	5.100	72.85	100	1
Hiprep 16/10 Q FF	0.125	3.349	26.79	65.66	367
Hiprep 16/60 S 300 HR	0.038	1.255	32.46	24.60	445

fast, high-yield recombinant protein production by large-scale infection of Sf9 cells.

Previous findings show that the productivity of hDPPIV/CD26 in the present study was approximately 80-fold higher than in related studies, even though the lower MOI value (0.1) reported in the published studies resulted in a ready procession to infection and production (Üstün-Aytekin et al., 2014). Dobers et al. (2002) reported productivity of hDPPIV/CD26 expression at 0.019 mU mL^{-1} h^{-1} at 48 h after infection with a recombinant baculovirus at a MOI of 0.7. In another work on the characterization and evaluation of recombinant DPPIV from Spodoptera frugiperda 21, the highest enzyme productivity was 0.04 mU mL^{-1} h^{-1} from 0.5×10^5 cell mL^{-1} using a MOI of 10 (Hsieh et al., 2011). A different study on recombinant human DPP8, which is similar to DPPIV, from a Sf9 cell line infected with a MOI of 0.5, had productivity of 0.044 mU mL^{-1} h^{-1}, according to Chen et al. (2004).

This result can be explained by the potential prevention of repeated serial passaging in the cell lines by using a lower MOI value. Therefore, no sharp decrease was observed in recombinant protein production, nor any increase in the viral passages. The use of low MOI on a large scale may extend the life span of stored viruses due to their 100–1000-fold lower consumption of virus inoculum per batch. Additionally, it may be possible to infect large fermenters directly from a frozen stock (Wasilko and Lee, 2006; Hsieh et al., 2011). These advantages of using low MOI promise the production of recombinant proteins in short time frames and with high productivity.

4.6. Separation processes of recombinant hDPPIV/CD26

The high- and low-molecular-weight contaminants, peptides, and amino acids were successfully removed in this chromatographic step. The recovery and resulting degrees of separation are summarized in Table 4. The fractions consisting of recombinant hDPPIV/CD26 were purified 445-fold with a yield of 24.6%, with respect to the initial culture, and the specific activity was almost 32.47 U mg^{-1}. Purification of hDPPIV/CD26 with immunoaffinity chromatography was used to overcome the bounding problem in cases in which the protein reassembled into a predominantly nonphysiological oligomeric form devoid of any enzymatic activity after elution. The reported specific activity of hDPPIV/CD26 in insect cells was 28.30 U mg^{-1}, and the yield was 19.8% (Dobers et al., 2002). These differences between activity and yield values are based on the utilization of different MOI titers and separation steps.

Cell maintenance and growth of healthy Sf9 cells play important roles in the determination of production parameters such as hDPPIV/CD26 expression in the baculoviral Sf9 cell system, optimal MOI, and infection time for the Sf9 cell line. Therefore, the preliminary experiment consisted of adapting the cells to a new medium (EX-CELL 420) and growing the adapted cells to a desired cell density on a small scale. Adapted and healthy cells were successfully subcultured and scaled up from a working volume of 1.5 L to a working volume of 3 L. It is clear that hydrodynamic parameters are crucial in terms of production; agitation and aeration without damaging shear-sensitive cells, bubble size, or gas consumption are difficult to achieve. These factors were determined for the Sf9 cell line, and a certain amount of serum was added to serum-free medium to decrease shear and stabilize the growth of insect cells in a stirred-tank fermenter.

Afterwards, the Sf9 cells were infected with baculovirus-infected cell stocks using a low multiplicity infection strategy in the fermenter. Thus, the present high productivity of hDPPIV/CD26 was derived. The other data collected by the study were acquired by monitoring the oxygen consumption of infected and uninfected Sf9 cells. Oxygen can be used by insect cells to provide energy for protein biosynthesis. For this reason, the positive relation between oxygen consumption and the level of expressed hDPPIV/CD26 was manifested in the present study.

The products of the gene were isolated using basic chromatography techniques. Thus, our use of certain production parameters for agitation without damaging shear-sensitive insect cells, in addition to sufficient gas transfer and expression of a high amount of DPPIV from Sf9 cells in a microbial fermenter has proven valuable in terms of the goals of the present study.

References

Aertgeerts K, Ye S, Tennant MG, Kraus ML, Rogers J, Sang BC, Skene RJ, Webb DR, Prasad GS (2004). Crystal structure of human dipeptidyl peptidase IV in complex with a decapeptide reveals details on substrate specificity and tetrahedral intermediate formation. Protein Sci 13: 412–421.

Agathos SN (1996). Insect cell bioreactors. Cytotechnology 20: 173–189.

Aiba S, Humphrey AE, Millis NF (1973). Biochemical Engineering. 2nd ed. London, UK: Academic Press.

Alam MNHZ, Razalı F (2005). Scale-up of stirred and aerated bioengineering bioreactor based on constant mass transfer coefficient. Jurnal Teknologi 43: 95–110.

Bailey JE, Ollis DF (1986). Biochemical Engineering Fundamentals. 2nd ed. New York, NY, USA: McGraw Hill.

Bavarian F, Fan LS, Chalmers JJ (1991). Microscopic visualization of insect cell-bubble interactions. Rising bubbles, air-medium interface, and the foam layer. Biotechnol Progr 7: 140–150.

Beas-Catena A, Sanchez-Miron A, Garcia-Camacho F, Contreras-Gomez A, Molina-Grima E (2013). Adaptation of the *Spodoptera exigua* Se301 insect cell line to grow in serum-free suspended culture. Comparison of SeMNPV productivity in serum-free and serum-containing media. Appl Microb Biotechnol 97: 3373–3381.

Bergmann A, Bohuon C (2002). Decrease of serum dipeptidylpeptidase activity in severe sepsis patients: relationship to procalcitonin. Clin Chim Acta 321: 123–126.

Carmo ACV, Giovanni DNS, Corrêa T, Martins LM, Stocco R, Suazo CAT, Mendonça RZ (2012). Expression of an antiviral protein from *Lonomia obliqua* hemolymph in baculovirus/insect cell system. Antivir Res 94: 126–130.

Celis JE, Carter N, Simons K, Small JV, Hunter T, Shotton D (2005). Cell Biology. 4th ed. Waltham, MA, USA: Elsevier Academic Press.

Chen YS, Chien CH, Goparaju CM, Hsu JTA, Liang PH, Chen X (2004). Purification and characterization of human prolyl dipeptidase DPP8 in Sf9 insect cells. Protein Expres Purif 35: 142–146.

Chisti Y (2000). Animal-cell damage in sparged bioreactors. Trends Biotechnol 18: 420–432.

Cunningham DF, O'Connor B (1997). Proline specific peptidases. BBA-Protein Struct M 1343: 160–186.

Demuth H, Heins J (1995). Catalytic mechanism of dipeptidyl peptidase IV. In: Fleischer RG, editor. Dipeptidyl Peptidase IV (CD26) in Metabolism and the Immune Response. Heidelberg, Germany: Springer-Verlag.

Dobers J, Zimmermann-Kordmann M, Leddermann M, Schewe T, Reutter W, Fan H (2002). Expression, purification, and characterization of human dipeptidyl peptidase IV/CD26 in Sf9 insect cells. Protein Expres Purif 25: 527–532.

Doran MP (1995). Bioprocess Engineering Principles. San Diego, CA, USA: Academic Press.

Doumas A, Van Den Broek P, Affolter M, Monod M (1998). Characterization of the prolyl dipeptidyl peptidase gene (dppIV) from the koji mold *Aspergillus oryzae*. Appl Environ Microb 64: 4809–4815.

Eibl R, Eibl D, Pörtner R, Catapano G, Czermak P (2009). Cell and Tissue Reaction Engineering. Berlin-Heidelberg, Germany: Springer-Verlag.

Garcia-Briones MA, Chalmers JJ (1992). Cell bubble interactions: mechanisms of suspended cell damage. Ann NY Acad Sci 665: 219–229.

Gomez E, Santos VE, Alcon A, Garcia-Ochoa F (2006). Oxygen transport rate on *Rhodococcus erythropolis* cultures: effect on growth and BDS capability. Chem Eng Sci 61: 4595–4604.

Handa A, Emery AN, Spier RE (1987). On the evaluation of gas-liquid interfacial effects on hybridoma viability in bubble column bioreactors. Dev Biol Stand 66: 241–253.

Hensirisak P, Parasukulsatid P, Agblevor FA, Cundiff JS, Velander WH (2002). Scale-up of microbubble dispersion generator for aerobic fermentation. Appl Biochem Biotechnol 101: 211–227.

Hsieh SK, Tzen JT, Wu TY, Chen YJ, Yang WH, Huang CF, Hsieh FC, Jinn TR (2011). Functional expression and characterization of dipeptidyl peptidase IV from the black-bellied hornet *Vespa basalis* in Sf21 insect cells. Biosci Biotech Biochem 75: 2371–2375.

Ikonomou L, Schneider YJ, Agathos S (2003). Insect cell culture for industrial production of recombinant proteins. Appl Microb Biotechnol 62: 1–20.

Iwaki-Egawa S, Watanabe Y, Kikuya Y, Fujimoto Y (1998). Dipeptidyl peptidase IV from human serum: purification, characterization, and N-terminal amino acid sequence. J Biochem 124: 428–433.

Jianyong Wu GK, Daugulis AJ, Faulkner P, Bone DH, Goosen MFA (1990). Adaptation of insect cells to suspension culture. J Ferment Bioeng 70: 90–93.

Kioukia N, Nienow AW, Emery AN, Al-Rubeai M (1995). Physiological and environmental factors affecting the growth of insect cells and infection with baculovirus. J Biotechnol 38: 243–251.

Laemmli UK (1970). Cleavage of structural proteins during the assembly of the head of bacteriophage T4. Nature 227: 680–685.

Lambeir AM, Proost P, Scharpé S, Meester ID (2002). A kinetic study of glucagon-like peptide-1 and glucagon-like peptide-2 truncation by dipeptidyl peptidase IV, in vitro. Biochem Pharmacol 64: 1753–1756.

Langford WS (2000). A comprehensive guide to managing autism. In: The Autism File. Special Supplement, London.

Lloyd RJ, Pritchard GG (1991). Characterization of X-prolyl dipeptidyl aminopeptidase from *Lactococcus lactis* subsp. *lactis*. J Gen Microbiol 137: 49–55.

Öngen G, Sargın S, Üstün Ö, Kutlu C, Yücel M (2012). Dipeptidyl peptidase IV production by solid state fermentation using alternative fungal sources. Turk J Biol 36: 665–671.

Ota T, Itoh A, Tachi H, Kudoh K, Watanabe T, Yamamoto Y, Tadahiro T, Maekawa A (2005). Synthesis of morphiceptin (Tyr-Pro-Phe-Pro-NH2) by dipeptidyl aminopeptidase IV derived from *Aspergillus oryzae*. J Agr Food Chem 53: 6112–6116.

Palomares LA, Ramirez O (1996). The effect of dissolved oxygen tension and the utility of oxygen uptake rate in insect cell culture. Cytotechnology 22: 225–237.

Pérez-Guzmán AE, Cruz y Victoria T, Cruz-Camarillo R, Hernández-Sánchez H (2004). Improvement of fermentation conditions for the production of X-prolyl-dipeptidyl aminopeptidase from *Lactococcus lactis*. World J Microb Biot 20: 413–417.

Pham PL, Perret S, Doan HC, Cass B, St-Laurent G, Kamen A, Durocher Y (2003). Large-scale transient transfection of serum-free suspension-growing HEK293 EBNA1 cells: peptone additives improve cell growth and transfection efficiency. Biotechnol Bioeng 84: 332–342.

Radner S, Celie PHN, Fuchs K, Sieghart W, Sixma TK, Stornaiuolo M (2012). Transient transfection coupled to baculovirus infection for rapid protein expression screening in insect cells. J Struct Biol 179: 46–55.

Reichelt K, Hole K, Hamberger A, Saelid G, Edminson P, Braestrup C, Lingjaerde O, Ledaai P, Orbeck H (1981). Biologically active peptide-containing fractions in schizophrenia and childhood autism. Adv Biochem Psychoph 28: 627–643.

Reichelt K, Knivsberg A (2003). Can the pathophysiology of autism be explained by the nature of the discovered urine peptides? Nutr Neurosci 6: 19–28.

Reuveny SKC, Eppstein L, Shiloach J (1992). Carbohydrate metabolism in insect cell cultures during cell growth and recombinant protein production. Ann NY Acad Sci 665: 220–237.

Rice JW, Rankl NB, Gurganus TM, Marr CM, Barna JB, Walters MM, Burns DJ (1993). A comparison of large-scale Sf9 insect cell growth and protein production: stirred vessel vs. airlift. Biotechniques 15: 1052–1059.

Schmid G (1996). Insect cell cultivation: growth and kinetics. Cytotechnology 20: 43–56.

Shattock P, Kennedy A, Rowell F, Berney T (1990). Role of neuropeptides in autism and their relationships with classical neurotransmitters. Brain Dysfunct 3: 328–345.

Tachi H, Ito H, Ichishima E (1992). An X-prolyl dipeptidyl-aminopeptidase from *Aspergillus oryzae*. Phytochemistry 31: 3707–3709.

Tanaka T, Camerini D, Seed B, Torimoto Y, Dang N, Kameoka J, Dahlberg HN, Schlossman SF, Morimoto C (1992). Cloning and functional expression of the T cell activation antigen CD26. J Immunol 149: 481–486.

Thoma R, Löffler B, Stihle M, Huber W, Ruf A, Hennig M (2003). Structural basis of proline-specific exopeptidase activity as observed in human dipeptidyl peptidase-IV. Structure 11: 947–959.

Tramper J, Vlak JM, Gooijer CD (1996). Scale up aspects of sparged insect-cell bioreactors. Cytotechnology 20: 221–229.

Urade M, Uematsu T, Mima T, Ogura T, Matsuya T (2006). Serum dipeptidyl peptidase (DPP) IV activity in hamster buccal pouch carcinogenesis with 9, 10-dimethyl-1, 2-benzanthracene. J Oral Pathol Med 21: 109–112.

Üstün Ö, Öngen G (2012). Production and separation of dipeptidyl peptidase IV from *Lactococcus lactis*: scale up for industrial production. Bioproc Biosyst Eng 35: 1417–1427.

Üstün-Aytekin Ö, Gürhan ID, Ohura K, Imai T, Öngen G (2014). Monitoring of the effects of transfection with baculovirus on Sf9 cell line and 1 expression of human dipeptidyl peptidase IV. Cytotechnology 66: 159–168.

Wasilko DJ, Lee SE (2006). TIPS: titerless infected-cells preservation and scale-up. Bioprocess J 5: 29–32.

Wasilko DJ, Edward LS, Stutzman-Engwall KJ, Reitz BA, Emmons TL, Mathis KJ, Bienkowski MJ, Tomasselli AG, David FH (2009). The titerless infected-cells preservation and scale-up (TIPS) method for large-scale production of NO-sensitive human soluble guanylate cyclase (sGC) from insect cells infected with recombinant baculovirus. Protein Expres Purif 65: 122–132.

Wilkinson RE, Houston DB (2001). Compositions containing dipepitidyl peptidase IV and tyrosinase or phenylalaninase for reducing opioid-related symptoms. US Patent 6251391.

Wu J, Goosen FA (1995). Evaluation of the killing volume of gas bubbles in sparged animal cell culture bioreactors. Enzyme Microb Tech 17: 1036–1042.

Yamaji H, Tagai S, Fukuda H (1999). Optimal production of recombinant protein by the baculovirus-insect cell system in shake-flask culture with medium replacement. J Biosci Bioeng 87: 636–641.

Zevaco C, Monnet V, Gripon JC (1990). Intracellular X-prolyl dipeptidyl peptidase from *Lactococcus lactis* spp. *lactis*: purification and properties. J Appl Microbiol 68: 357–366.